Journal of Peptide Science
J. Pept. Sci. 2007; **13**: 171–178
Published online 31 January 2007 in Wiley InterScience (www.interscience.wiley.com). DOI: 10.1002/psc.828

JOURNAL OF PEPTIDE SCIENCE

A synthetic analog of plantaricin 149 inhibiting food-borne pathogenic bacteria: evidence for α-helical conformation involved in bacteria–membrane interaction

DIANA M. MÜLLER,[a] MARTA S. CARRASCO,[b] ARTURO C. SIMONETTA,[b] LEILA M. BELTRAMINI[c] and GEORGINA G. TONARELLI[a]*

[a] Departamento de Química Orgánica, Facultad de Bioquímica y Cs. Biológicas, Universidad Nacional del Litoral (U.N.L). Ciudad Universitaria, Santa Fe, Argentina
[b] Cátedras de Microbiología y Biotecnología, Departamento de Ingeniería en Alimentos, Facultad de Ingeniería Química, Universidad Nacional del Litoral (U.N.L). Santiago del Estero 2829, Santa Fe, Argentina
[c] Departamento de Física e Informática, Grupo de Biofísica Molecular Sérgio Mascarenhas, Instituto de Física de São Carlos-São Paulo, Brazil

Received 1 August 2006; Accepted 2 November 2006

Abstract: Plantaricin-149 is a bacteriocin produced by *Lactobacillus plantarum* NRIC 149 (a LAB isolated from pineapple), which consists of a peptidic chain made up of 22 amino acid residues [Kato *et al. J. Ferment. Bioeng.* 1994; **77**: 277–282]. In this work, a synthetic *C*-terminal amidated peptide analog denoted Pln149a was prepared by SPPS-Fmoc chemistry and the antagonistic activity against gram-positive and gram-negative bacteria was tested. The secondary structure was studied by circular dichroism (CD) and the vicinity of the tyrosine residue by fluorescence spectroscopy under different conditions. We report the results of the interaction of Pln149a with reverse micelles prepared from the amphiphilic AOT in cyclohexane.

Synthetic plantaricin was active against one strain of *Staphylococcus aureus* and four strains of *Listeria* genus at pH 5.5 and 7.4 and, like its natural variant, inhibited *L. plantarum* ATCC 8014.

The data derived from spectroscopic measurements in presence of AOT reverse micelles suggest that the secondary structure of the peptide upon interaction is an α-helix. In this membrane model, the hydrophobic side of the α-helix is inserted into the micelles, leaving the lysines exposed to the solvent and interacting with the polar moieties of AOT. The fluorescence data point out that the *N*-terminal tyrosine residue is close to the micellar interface. Copyright © 2007 European Peptide Society and John Wiley & Sons, Ltd.

Keywords: bacteriocin; plantaricin 149; circular dichroism; tyrosine fluorescence; α-helix

INTRODUCTION

LAB are known to secrete antimicrobial polypeptides, termed *bacteriocins*. The family of bacteriocins includes a diversity of peptides in terms of size, primary and secondary structure, and microbial targets [1–4]. The use of bacteriocins from LAB to control the growth of *Listeria monocytogenes* and *Staphylococcus aureus* is attractive to the dairy and food industries because of the increasing consumer demand for natural products and the growing concern about food-borne illness. Consequently, with the potential applications of bacteriocins as food biopreservatives, detailed insights at a structural level may contribute to a better understanding of their mode of action.

Among LAB, there has been much interest in *Lactobacillus plantarum* strains, owing to their potential application as starter bacteria for the fermentation of vegetables, meat, and fish products [5]. Some bacteriocins from *L. plantarum* have been isolated and partially characterized. However, only a few have been purified and sequenced. With the exception of plantaricin A [6], plantaricin E/F, plantaricin J/K [7], and plantaricin C [8], information on the secondary structure of *L. plantarum* bacteriocins is still scarce.

L. plantarum C11 produce three variants of plantaricin A (PlnA) of 26, 23, and 22 amino acid residues, all of which show antimicrobial and pheromonal activity. The inhibition spectrum of PlnA-22 is particularly directed against *L. plantarum* C11 closely related strains like *L. plantarum, L. casei, L. sake, Pediococcus pentosaceus*, and *Carnobacterium piscicola* [6,9].

Plantaricin 149 is a bacteriocin produced by *L. plantarum* NRIC 149 isolated from pineapple, and its molecular weight was estimated to be 2.2 kDa by SDS-PAGE. By *N*-terminal amino acid sequence analysis, 22 amino acid residues were identified: YSLQMGATAIKQVKKLFKKKGG. The spectrum of inhibitory activity of plantaricin 149 includes genera, species and subspecies of LAB, such as *L. plantarum, Lactobacillus delbrueckii* subsp. *delbrueckii, L. delbrueckii* subsp.

Abbreviations: AOT, sodium-bis-(2-ethylhexyl)-sulfosuccinate; CD, circular dichroism; LAB, lactic acid bacteria; SELCON, self-consistent method.

*Correspondence to: G. G. Tonarelli, Departamento de Química Orgánica, Facultad de Bioquímica y Ciencias Biológicas, UNL. Ciudad Universitaria. C.C.242 (3000), Santa Fe, Argentina;
e-mail: tonareli@fbcb.unl.edu.ar

bulgaricus, Lactobacillus helveticus, Lactobacillus casei, Leuconostoc mesenteroides, *Pediococcus acidilactici*, *P. cerevisiae, Enterococcus hirae* and *Lactococcus*. The bacteriocin did not inhibit other gram-positive and gram-negative bacteria [10].

Peptide–membrane interactions of many bacteriocins involve adsorption and structuring of the soluble random-coil peptide in an α-helical form at the membrane surface, followed by insertion of the helix into the membrane and association with other peptides to generate its active form [11,12]. For PlnA peptides it was found that the antimicrobial activity is mediated through the formation of an amphiphilic α-helical structure [6,9]. However, the plantaricin 149 structure has been poorly characterized previously, and its mode of action is unknown.

In the present study, a synthetic *C*-terminal carboxamide analog of plantaricin 149, denoted Pln149a was prepared by SPPS. Its antagonistic activity against several food-borne pathogenic bacteria was investigated, and the secondary structure characterized by CD and fluorescence spectroscopy, under various experimental conditions. The relevance of Pln149a bactericidal activity against *S. aureus* and *Listeria* strains and the structural data revealing that an α-helical conformation is involved in bacteria–membrane interaction will be discussed in detail.

MATERIALS AND METHODS

Synthesis and Purification of Pln149a

Pln149a was chemically synthesized according to the amino acid sequence reported earlier (YSLQMGATAIKQVKKLFKKKGG) [10]. It was prepared by the solid-phase method following Fmoc chemistry. Rink amide 4-methylbenzydrylamine (MBHA) resin was used to prepare the *C*-terminal peptide amide. Couplings were performed by PyBOP, and NMM was used as the catalyst; Fmoc-deblockings were done with 20% piperidine in DMF (v/v).

Final cleavage from the resin was achieved by a mixture of TFA/H_2O/EDT/TIS (94.5 : 2.5 : 2.5 : 0.5) (v/v). After 3 h, the resin was filtered off, and the crude peptide was precipitated in dry cold diethyl ether, centrifuged, and washed several times with cold diethyl ether until scavengers were removed. The product was then dissolved in water and lyophilized twice.

The crude peptide was dissolved in H_2O (0.1% TFA) (5 mg/ml) and purified by semipreparative reverse-phase HPLC on a Gilson equipment (USA) in a Vydac 218TP1010 (C_{18}, 5 μm, 300 Å, 10 mm i.d. × 250 mm) column, using gradients of (B) MeCN in (A) H_2O both containing 0.1% TFA. Peptides were separated by the following gradient: 10–25% B over 5 min, then 25–40% B over 20 min and 40–60% B over 5 min. The eluates were monitored by their UV absorbance at 220 nm. The purified peptide was analyzed by RP-HPLC on a Delta Pak C_{18} analytical (5 μm, 300 Å, 3.9 × 150 mm, Waters) column, using similar running conditions as described above.

MALDI-TOF Analysis

MALDI-TOF mass analysis was done on a Voyager-DE STR Biospectrometry workstation (Perseptive Biosystems). The instrument is equipped with a nitrogen laser operating at 337 nm. All the experiments were performed using α-cyano-4-hydroxycinnamic acid as the matrix. MALDI-TOF spectra were calibrated externally using a mixture of peptide standards Cal Mix 1 and 2 (Applied Biosystems).

Amino Acid Sequencing

The peptide amino acid sequence was confirmed by automatic Edman degradation, performed on a Shimadzu PPSQ-23 A sequencer.

Antimicrobial Activity Assays

Bacterial strains and culture conditions. The following bacterial strains, belonging to the collection of the Food Engineering Department (Microbiology and Biotechnology Sections), FIQ, Universidad Nacional del Litoral, Argentina, were used as indicators of Pln149a antimicrobial activity: four strains of *L. plantarum* identified as DBFIQ LP 22, DBFIQ LP 28, DBFIQ LP 38, and DBFIQ LP 41; *L. delbrueckii* subsp. *bulgaricus* DBFIQ LB 42; *Pseudomonas* sp. DBFIQ P 55; *S. aureus* DBFIQ S 21; *L. monocytogenes* DBFIQ LM 3; *Bacillus cereus* DBFIQ B 28; four strains of the *Enterococcus* genus identified as DBFIQ E 13, DBFIQ E 23, DBFIQ E 24 and DBFIQ E 25. Other strains used as indicators were: *Lactococcus lactis* subsp. *lactis* CRL G3, from the collection of the Center for Lactobacillus Reference Strains (CERELA, Tucumán, Argentina); *L. plantarum* ATCC 8014, from the American Type Culture Collection; and finally, three strains of *L. mesenteroides* subsp. *dextranicum* identified as NCDO 529, DTUNLu 223, and DTUNLu 245, *L. mesenteroides* subsp. *cremoris* NCDO 543, *L. monocytogenes* type I DTUNLu 328, *L. monocytogenes* DTUNLu 335 BsAs, and *Listeria seeligeri* DTUNLu 340, all of them belonging to the collection of the Technology Department, Universidad Nacional de Luján, Argentina.

The different strains were lyophilized and also frozen at −20 °C in Nutrient Broth (Merck) for nonlactic bacteria, and in MRS Broth (Merck) or M17 Broth (Merck) for LAB, supplemented with 15% (v/v) glycerol for cryoprotection. Before their use, the nonlactic bacteria were propagated overnight at 37 °C in Nutrient Broth (Merck), while LAB were propagated in MRS Broth (Merck) or in M17 Broth (Merck).

Detection of Antagonistic Activity

The agar-well diffusion assay was used to investigate the antimicrobial activity of Pln149a [13]. For this purpose, 1 ml of an overnight culture of each indicator strain was added to 19 ml of molten Nutrient Agar (Difco) and poured into a sterile Petri dish. After cooling, wells of 7-mm diameter were cut into the agar plates and filled with 80 μl of Pln149a aqueous solution, 420 μM, pH 5.5. The plates were incubated at 37 °C for 24 h and the diameters of the clear inhibition zones were subsequently measured. The antimicrobial activity against *L. monocytogenes* DBFIQ LM 3 *and S. aureus* DBFIQ S 21 was

DOI: 10.1002/psc

also tested in 50 mM phosphate buffer, pH 7.4. Each assay was done in triplicate and the results were expressed as the average of the measured values.

The titer of bacteriocin activity against *L. monocytogenes* DBFIQ LM 3 and *S. aureus* DBFIQ S 21 strains was expressed as a arbitrary units (AU). One AU was defined as the reciprocal of the highest dilution of the bacteriocin that showed a distinct zone of inhibition of the indicator strains [13,14].

Mode of Action

In order to study the antimicrobial effect of Pln149a on *L. monocytogenes* DBFIQ LM 3 and *S. aureus* DBFIQ S 21 strains, 1 ml of 840 μM peptide solution in 50 mM phosphate buffer, pH 7.4 was added to 10 ml of log-phase cultures in Nutrient Broth (Merck), with initial cellular concentration of 10^7 CFU ml^{-1}. The number of viable cells was determined at intervals of 2 h 30 min and during 24 h, by a direct counting method in Petri dishes. Control cultures were prepared by adding 1 ml of 50 mM phosphate buffer pH 7.4 to 10 ml of a log-phase culture of each indicator microorganism in Nutrient Broth (Merck). Each assay was performed in triplicate and the results expressed as the average of the measured values [14,15].

Minimal Inhibitory Concentration (MIC) Determination

Minimal inhibitory concentration (MIC) determinations were performed using the modified microtiter dilution assay, according to the procedures proposed by the R.E.W. Hancock Laboratory for testing antimicrobial peptides; polypropylene 96-well plates were used and incubated for 18 h at 37 °C. *L. monocytogenes* DBFIQ LM 3 and *S. aureus* DBFIQ S 21 strains were cultured on Mueller–Hinton Broth (Biokar Diagnostics). The considered MIC was the lowest drug concentration that reduced growth by >50% compared with the growth in the control well [16–18].

Hemolysis Assay

The hemolytic activity of the peptides was evaluated essentially as described earlier [19]. Human erythrocytes were isolated by centrifugation from freshly collected blood, and washed three times with isotonic-saline solution. An aliquot of 0.5 ml of a suspension containing approximately 10^5 cells ml^{-1} was incubated under stirring at 37 °C for 1 h with 1 ml of peptide solutions, at concentrations ranging from 25 to 500 μg ml^{-1}. The solutions were centrifuged, and the absorbance of the supernatant was measured at 540 nm. A value of 100% cell lysis was determined by incubation of erythrocytes in the presence of 1% Triton X-100.

Far-UV Circular Dichroism

Far-UV CD spectra (190–250 nm) were recorded at 25 °C in a Jasco J715 instrument (Jasco Corporation, Japan), using cylindrical quartz cells of 1 mm path length, with 30 μM Pln149a in water, 20, 40, and 80% of TFE, phosphate buffer pH 5.5 and pH 7.4, either in the absence or in the presence of AOT reverse micelles solution. All the spectra were recorded after accumulation of 16 scans. The CD spectra of micelle solutions were subtracted to eliminate background effects. Quantitative prediction of the secondary structure was performed by deconvolution of the CD spectra using the Selcon program developed by Sreerama and Woody [20,21].

Fluorescence Studies

Steady-state fluorescence spectra (280–400 nm) of 20 μM Pln149a in buffer and AOT reverse micelles were obtained at 25 °C in an ISS spectrofluorometer (Hitachi, Japan) using rectangular quartz cuvettes of 1 cm path length with optical density values <0.07–0.08 to avoid inner filter effects. The interaction with reverse micelles was studied by the changes in tyrosine fluorescence of the peptide with excitation at 275 nm. The fluorescence spectra of micelles and buffer solutions were subtracted to eliminate scattering effects.

Reverse Micelle Preparation

Reverse micelles were prepared by the injection method [22]. For this, small aliquots of a stock peptide solution (1 mM in 50 mM phosphate buffer, pH 7.4) were added to a surfactant/organic solvent solution (50 mM AOT/cyclohexane). All the volume injected was considered as water and was used to calculate $W_0 = [H_2O]/[AOT]$. Reverse micelles with $W_0 = 16$ were prepared by adding 15 μl of concentrated peptide solution to 1 ml of 50 mM AOT/cyclohexane solution, followed by shaking until clear (final peptide concentration 15 μM) [23]. In the experiments, we have used micelles with $W_0 > 10$ to eliminate AOT packing constraints [24]. The concentration of the amphiphiles was always in large excess compared to that of Pln149a; the molar ratio of peptide/surfactant was 1/3333 (mol/mol) when W_0 was set to 16.

Blank samples of micelles in buffer were prepared using the same protocol as described, to eliminate background effects of micelles in the spectroscopic measurements.

Hydrophobicity Calculations

Peptide hydrophobicity (H) and hydrophobic moments (μH) were calculated using the normalized consensus hydrophobicity scale of Eisenberg [25] and The European Molecular Biology Open Software Suite (EMBOSS) [26], with a window size of ten residues.

RESULTS AND DISCUSSION

Analysis by MS

The theoretical mass to charge ratio for M^+ of Pln149a is 2423.96 (average mass). The experimental values of MH^+, MNa^+, and MK^+ were observed at m/z 2424.9, 2446.8, and 2462.6, respectively (Figure 1).

Antimicrobial and Hemolytic Activities

The inhibitory spectrum of Pln149a is shown in Table 1. The peptide showed inhibitory effect against 6 of the 22 tested strains. Interestingly, it effectively inhibited all the tested *Listeria* strains and the strain of *S. aureus*

DOI: 10.1002/psc

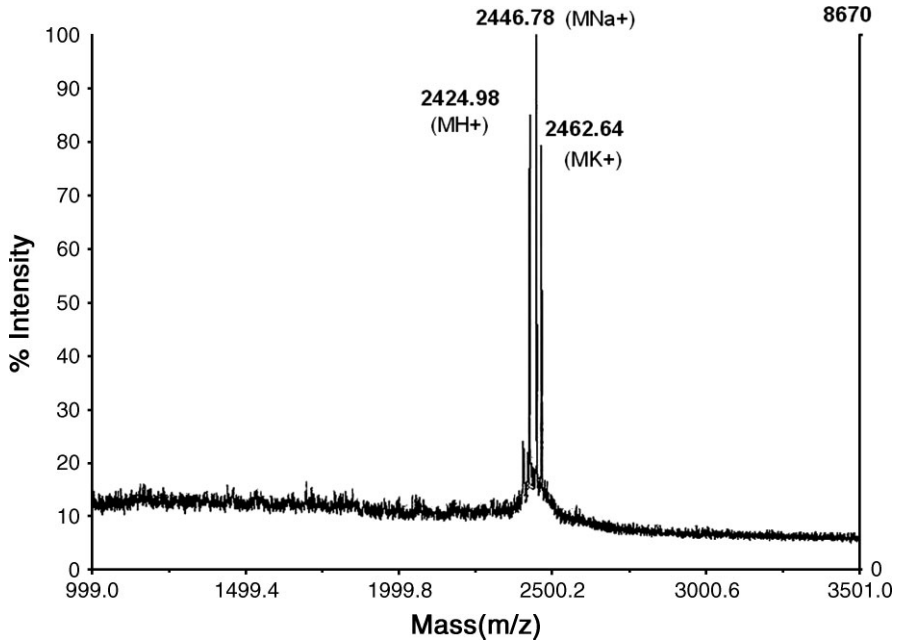

Figure 1 MALDI-TOF Mass spectrometry of Pln149a. The experimental values of MH^+, MNa^+, and MK^+ were observed at m/z 2424.9, 2446.8, and 2462.6 respectively.

Table 1 Inhibitory spectrum of Pln149a (420 μM) determined by the well diffusion assay

Indicator strains	Diameter of inhibition zone (mm), pH = 5.5	Diameter of inhibition zone (mm), pH = 7.4
L. plantarum [c]ATCC 8014	1	NA
Staphylococcus aureus [a]DBFIQ S 21	5	5
Listeria monocytogenes [a]DBFIQ LM 3	2	3.5
L. monocytogenes [b]DTUNLu 335 BsAs	3.5	4
L. monocytogenes tipo I [b]DTUNLu 328	1	1
Listeria seeligeri [b]DTUNLu 340	1	1

Diameter of inhibition zone (mm): the diameter of the wells (7 mm) was subtracted from the inhibited zone.
NA: Not assayed.
[a] DBFIQ: Collection of Cátedras de Microbiología y Biotecnología-FIQ, Univ. Nac. del Litoral, Argentina.
[b] DTUNLu: Collection of Departamento de Tecnología, Univ. Nac. de Luján, Argentina.
[c] ATCC: American Type Culture Collection.

(coagulase-positive) at both pH 5.5 and 7.4. The titer of antimicrobial activity against these gram-positive pathogenic bacteria was 100 AU ml^{-1} (125 μg ml^{-1}), as determined by the agar-well diffusion assay. However, among the *Lactobacillus* strains, only *L. plantarum* ATCC 8014 was inhibited by Pln149a at pH 5.5 (pH 7.4 was not assayed).

In order to determine whether the mode of action of Pln149a was bactericidal or bacteriostatic, the viability of *S. aureus* DBFIQ S 21 and *L. monocytogenes* DBFIQ LM 3 was monitored in the presence of the peptide (final concentration: 74.5 μM, pH 7.4). It was found that the addition of Pln149a to log-phase cultures of *L. monocytogenes* and *S. aureus* decreased the number of viable cells per milliliter from 1×10^7 to below 10^2 CFU after incubation for 6 h, whereas in the control broth, the number of viable cells increased progressively from 1×10^7 up to approximately 3.6×10^8 CFU ml^{-1} after 24 h incubation (Figure 2). Therefore, these results clearly prove the bactericidal activity of Pln149a against these strains of gram-positive food-borne pathogens *L. monocytogenes* and *S. aureus*.

The MIC of Pln149a against *L. monocytogenes* DBFIQ LM 3 and *S. aureus* DBFIQ S 21 was also determined using the modified microtiter dilution assay, according to the procedures proposed by the R.E.W. Hancock Laboratory for testing antimicrobial peptides. Unexpectedly large MIC values were found for Pln149a against *L. monocytogenes* (264 μM) and *S. aureus* (528 μM) when using full-strength Mueller–Hinton broth medium. A possible explanation for this finding is that the peptide interacts strongly with components of the Mueller–Hinton broth medium and so its activity is reduced in these assays. A medium-dependent antimicrobial activity (MIC) for antimicrobial peptides has been reported when assayed in Mueller–Hinton broth of different strengths [27,28].

DOI: 10.1002/psc

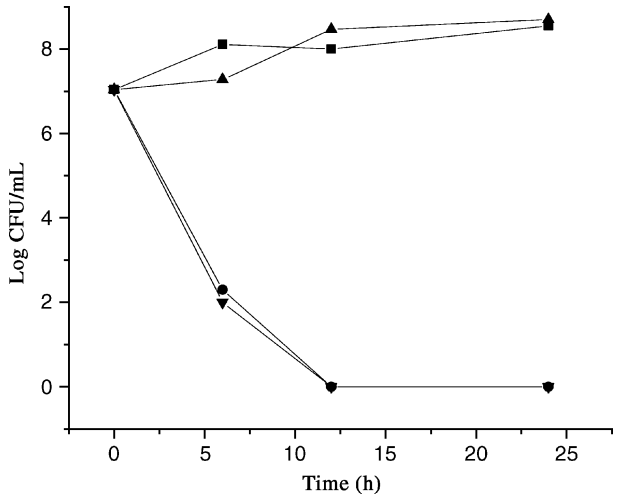

Figure 2 Bactericidal effect of Pln149a against cultures of *L. monocytogenes* and *S. aureus* strains. Peptide concentration: 74.5 μM, pH 7.4; (■) control culture of *L. monocytogenes*; (●) *L. monocytogenes* after addition of Pln149a; (▲) control culture of *S. aureus;* (▼) *S. aureus* after addition of Pln149a.

Pln149a showed low hemolytic activity (16%) in the whole range of concentrations (25–400 μg ml^{-1}) used, suggesting its selectivity against bacterial membranes.

Secondary Structure

The CD results showed that Pln149a adopts a random structure in water and in phosphate buffer at pH 7.4 and 5.5, as expected for a small peptide in aqueous solutions. The deconvolution of the Pln149a spectrum confirmed the high content of unordered structure (83%) compared to other structures (17%), consistent with the pronounced CD minimum about 198 nm (Figure 3). This large content of unordered structure required the use of a special reference set of 48 proteins that included spectra from denaturated proteins for deconvolution [29].

The presence of different TFE concentrations induced an increase of helical elements, as shown by the appearance of two minima at about 206 and 223 nm, and a maximum at 190 nm (Figure 3). The deconvolution of these spectra using the CDpro package (SELCON3, CONTINLL, CDSSTR) indicated 37% helix and 60% unordered structure in 20% TFE while >90% helical element was estimated in 80% TFE [30].

Pln149a in the presence of AOT reverse micelles ($W_0 = 16$) also adopted a folded secondary structure, with the same two negative minima at 206 and 222 nm, and a maximum at 194 nm, mainly associated to the transitions found in helical structures [31]. The deconvolution results pointed to an increase in helical content to about 70%, followed by a decrease in the unordered content (about 30%). When binding to AOT reverse micelles, Pln149a adopted a helical structure similar to that reported for PlnA-22 upon exposure to TFE, anionic DOPG liposomes, DPC, and SDS micelles [9].

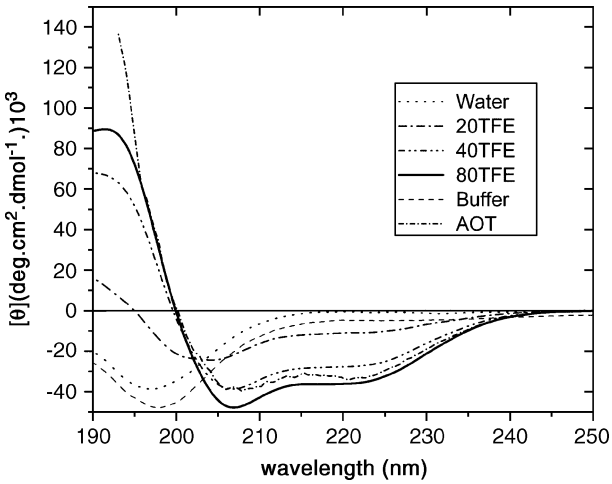

Figure 3 CD spectra of Pln149a. In water; phosphate buffer, pH 7.4; 20, 40, and 80% TFE (peptide concentration: 30 μM); and in the presence of AOT reverse micelles, pH 7.4 ($W_0 = 16$). The spectra were recorded after accumulation of 16 scans.

Pln149a showed maximum fluorescence emission at 310 nm in phosphate buffer pH 7.4 and in the presence of AOT/cyclohexane reverse micelles ($W_0 = 16$), indicating a high degree of exposure of the tyrosine residue to the aqueous phase [32]. Nevertheless, the decrease in fluorescence intensity observed in the presence of micelles suggests that the peptide is interacting with the micelles and that this interaction affects the tyrosine (Figure 4). In reverse micelles with $W_0 = 20$, the modifications detected by fluorescence were small, suggesting that the location of the fluorophore was not affected by the increase in the water content of the micelles (data not shown).

AOT reverse micelles are commonly prepared using linear or cyclic saturated hydrocarbons as organic solvents. However, the characteristics of the apolar

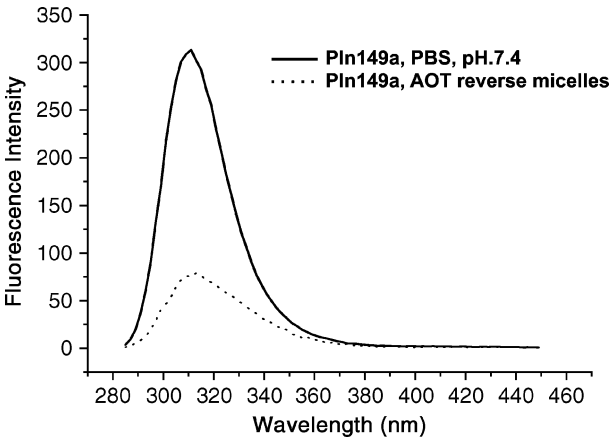

Figure 4 Fluorescence spectra of Pln149a. In phosphate buffer, pH 7.4 (peptide concentration: 20 μM); and in the presence of AOT reverse micelles ($W_0 = 16$, peptide concentration: 15 μM). The excitation wavelength was 275 nm, and the emission was scanned from 280 to 400 nm.

DOI: 10.1002/psc

solvent influence the properties of the micellar interface by a solvation effect [33–35]. Recent studies have demonstrated that the interaction between a protein and the micellar interface is a dominant factor influencing the protein structure in reverse micelles [36]. New spectroscopic studies of PLn149a in the presence of AOT/linear hydrocarbons micelles may be carried out to explore the effect of organic solvents on the secondary structure of the peptide.

The Structure/Activity Relationship of Pln149a

Plantaricin 149 is a highly cationic 22-mer peptide that shares a significant sequential homology with PlnA-22. Both plantaricins differ at residues 20 and 22, corresponding to Trp20 and Trp22 in PlnA-22, *versus* Lys20 and Gly22 in plantaricin 149. It was found that the μH of PlnA-22 and Pln149 calculated by the Eisenberg equation [25,26] were very similar, 0.60 and 0.55 respectively. There is a small difference in H between the two plantaricins, 0.05 and −0.07 for PlnA-22 and Pln149, respectively.

A molecular model of the whole Pln149a sequence was obtained by the SP^3 software [37] and the structure visualization was done with PyMOL version 0.97 [38]. The predicted helical region extends from Ala7 to Lys20 (Figure 5(A)). The proposed helix stretching from residues 10–19 (IKQVKKLFKK), correspond to the most amphipathic region (μH 0.837) with the polar residues Lys11, Lys14, Lys15, Lys18, and Lys19 along one side of the helix and the nonpolar residues, Ile10, Val13, Leu16, and Phe17 along the other. A front view of region 10–19 is shown in Figure 5(B).

Most of host-defense peptides share the features of being positively charged under physiological conditions and are able to adopt an amphipathic α-helical or β-sheet structure upon association with lipid bilayers. Different studies suggest that cell specificity of antimicrobial peptides can be controlled by an optimal balance between H and the net positive charge [39–41]. Particularly, Pln149a sequence has a ratio of hydrophilic residues/total number of residues of 41% and contains six positively charged Lys residues (27%), which are spread along the whole sequence. We have used a *C*-terminal carboxamide analog of plantaricin 149 instead of the carboxylate-free peptide to increase the net charge of the peptide to +7. Amidation is a common post-translational modification that appears in a wide variety of antimicrobial peptides, such as melittin, cecropins, dermaseptins, PR-39, and other peptides isolated from animals. In several cases, synthetic *C*-terminally amidated analogs of peptides whose native forms are not amidated show increased antimicrobial activity [42].

Different model systems have been developed for studying the interaction of host-defense peptides with membranes, including multilamellar and unilamellar vesicles, planar lipid bilayers, lipid monolayers, micelles, and colorimetric biomimetic membranes [43,44].

In this work, we have used AOT reverse micelles as a membrane model system and CD and fluorescence spectroscopic methodologies to study the structural modifications of Pln149a following its interaction with the micelles. The results suggest that the hydrophobic side of the α-helix is inserted into the micelles, leaving the lysines exposed to the solvent and interacting with the polar moieties of AOT. Additionally, the analysis of the emission spectra of Pln149a in buffer and in the presence of AOT reverse micelles suggests that the *N*-terminal tyrosine residue is in the proximity of the micellar interface, where it interacts with the polar and hydrophobic moieties of the surfactant/cyclohexane system.

Two general mechanisms were originally proposed to describe the process of phospholipid membrane permeation by membrane-active peptides. These were the 'barrel–stave' mechanism [45] in which peptides insert into the hydrophobic core of the membrane and assemble to form a transmembrane pore, and the 'carpet' mechanism in which peptides bind the phospholipid membrane surface until a threshold concentration is reached, and then permeate it in

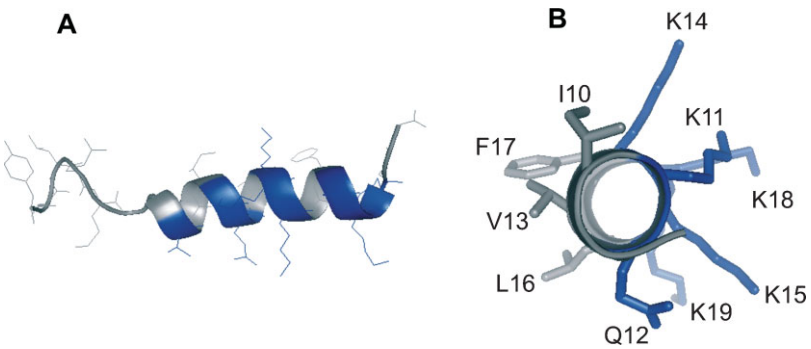

Figure 5 Molecular model of Pln149a obtained by the SP^3 1.0 software; PyMOL version 0.97 was used for structure visualization. The charged and polar residues of the helix are in blue and the hydrophobic ones in gray. (A) Side view of the Pln149a complete sequence. (B) Front view of region 10–19 (IKQVKKLFKK), corresponding to the most amphipathic helical region. Mean $\mu H = 0.837$.

DOI: 10.1002/psc

a detergent-like manner. According to the latter mechanism, the positively charged amino acids are spread along the peptidic chain and are continuously in contact with the lipid head group during the process of membrane permeation [40,46].

Our findings about the low hemolytic activity of Pln149a, its predominant amphipathic α-helical structure induced when binding AOT reverse micelles, and its cationic character are compatible with the 'carpet' mechanism proposed by Shai [40] to explain the mode of action of linear, cell-selective, amphipathic α-helical antimicrobial peptides. Nevertheless, recent studies about the interaction of PlnA with model membranes have evidenced that different mechanisms, 'carpet', 'toroidal pore', and a new mechanism proposed by the authors, 'leaky slit', could be involved in membrane perturbation by antimicrobial peptides [47].

As a consequence of recurring and serious listeriosis outbreaks, *L. monocytogenes* has come under the focus of bacteriocin investigators during the past decade. The most extensively studied bacteriocin, Nisin, is produced by *L. lactis* strains. The use of Nisin as a food additive was approved in 1969 by the joint Food and Agriculture Organization/World Health Organization (FAO/WHO). Its effectiveness against important gram-positive food-borne pathogens and spoilage agents has been widely documented. Nisin shows high solubility, antimicrobial activity, and thermostability at pH 2.0, but it is inactive and shows low solubility at pH 7.0 [48,49].

On the other hand, pediocin PA-1 that is produced by *P. acidilactici* PAC 1.0 has strong antilisterial activity and has been identified as a promising new candidate for food preservation. Pediocin PA-1 activity is affected by pH, and it is active at pH 6 but becomes inactive at pH 8 [50].

In most cases, plantaricins produced by different strains of *L. plantarum* are active against closely related strains of LAB; antimicrobial activity against *L. monocytogenes* has been reported for a few plantaricins like plantaricin C19 [51] and plantaricin D [52]. We have found that Pln149a was active against different *Listeria* strains. At this point, it is interesting to remark that for some *Listeria* strains the inhibitory activity of Pln149a was found to be similar at pH 5.5 and 7.4 but for some others it increased at pH 7.4 (Table 1). This finding adds to the technological interest in the molecule.

CONCLUSIONS

In conclusion, the bactericidal activity of Pln149a against strains of gram-positive, food-borne pathogens *L. monocytogenes* and *S. aureus* found in this work is a promising result that may be deeply explored in order to evaluate the potential biotechnological application of this bacteriocin for food preservation.

Acknowledgements

We thank Dr. David Andreu from Proteómica-Química de Proteínas, Universitat Pompeu Fabra, Barcelona, Spain, for the MALDI-TOF analysis and Dr María Cristina Mans from Departamento de Tecnología de la Universidad Nacional de Luján (UNLu), Argentina, for providing us with the *Listeria* and *Leuconostoc* strains.

REFERENCES

1. Tagg JR, Dajani AS, Wannamaker LW. Bacteriocins of gram-positive bacteria. *Bacteriol. Rev.* 1976; **40**: 722–756.
2. Klaenhammer TR. Bacteriocins of lactic acid bacteria. *Biochimie* 1988; **70**: 337–349.
3. Riley MA, Wertz JE. Bacteriocin diversity: ecological and evolutionary perspectives. *Biochimie* 2002; **84**: 357–364.
4. Schillinger U, Geisen R, Holzapfel WH. Potential of antagonistic microorganisms and bacteriocins for the biological preservation of food. *Trends Food Sci. Technol.* 1996; **7**: 158–164.
5. Mckay LL, Baldwin KA. Aplications for biotechnology: present and future improvements in lactic acid bacteria. *FEMS Microbiol. Rev.* 1990; **7**: 3–14.
6. Hauge HH, Mantzilas D, Moll GN, Konings WN, Driessen AJ, Eijsink VG, Nissen-Meyer J. Plantaricin A is an amphiphilic alpha-helical bacteriocin-like pheromone which exerts antimicrobial and pheromone activities through different mechanisms. *Biochemistry* 1998; **37**: 16026–16032.
7. Hauge HH, Mantzilas D, Eijsink VG, Nissen-Meyer J. Membrane-mimicking entities induce structuring of the two-peptide bacteriocins plantaricin E/F and plantaricin J/K. *J. Bacteriol.* 1999; **181**: 740–747.
8. Turner DL, Brennan L, Meyer HE, Lohaus C, Siethoff C, Costa HS, González B, Santos H, Suárez JE. Solution structure of plantaricin C, a novel lantibiotic. *Eur. J. Biochem.* 1999; **264**: 833–839.
9. Kristiansen PE, Fimland G, Mantzilas D, Niseen-Meyer J. Structure and mode of action of the membrane-permeabilizing antimicrobial peptide pheromone Plantaricin A. *J. Biol. Chem.* 2005; **280**: 22945–22950.
10. Kato T, Matsuda T, Ogawa E, Ogawa H, Kato H, Doi U, Nakamura R. Plantaricin-149 a bacteriocin produced by *Lactobacillus plantarum* NRIC 149. *J. Ferment. Bioeng.* 1994; **77**: 277–282.
11. Abee T. Pore-forming bacteriocins of gram-positive bacteria and self-protection mechanism of producer organisms. *FEMS Microbiol. Lett.* 1995; **129**: 1–10.
12. Hauge HH, Nissen-Meyer J, Nes IF, Eijsink VGH. Amphiphilic α-helices are important structural motifs in the α and β peptides that constitute the bacteriocin lactococcin G: enhancement of helix formation upon α-β interaction. *Eur. J. Biochem.* 1998; **251**: 565–572.
13. Tagg JR, Mcgiven AR. Assay systems for bacteriocins. *Appl. Environ. Microbiol.* 1971; **21**: 943–947.
14. Kang JH, Lee MS. Characterization of a bacteriocin produced by *Enterococcus faecium* GM-1 isolated from an infant. *J. Appl. Microbiol.* 2005; **98**: 1169–1176.
15. Simonetta AC, Moragues de Velasco LG, Frisón LN. Antibacterial activity of enterococci strains against *Vibrio cholerae*. *Lett. Appl. Microbiol.* 1997; **24**: 139–143.
16. Amsterdam D. Susceptibility testing of antimicrobials in liquid media. In *Antibiotics in Laboratory Medicine*, Lorian V (ed.). The Williams and Wilkins Co: Baltimore, 1996; 52–111.
17. Wu M, Hancock REW. Interaction of the cyclic antimicrobial cationic peptide bactenecin with the outer and cytoplasmic membrane. *J. Biol. Chem.* 1999; **274**: 29–35.
18. Steinberg DA, Hurst MA, Fujii CA, Kung AH, Ho JF, Cheng FC, Loury DJ, Fiddles JC. Protegrin-1: a broad-spectrum, rapidly

microbicidal peptide with in vivo activity. *Antimicrob. Agents Chemother.* 1997; **41**: 1738–1742.
19. Sitaram N, Nagaraj R. A synthetic 13-residue peptide corresponding to the hydrophobic region of bovine seminalplasmin has antibacterial activity and also causes lysis of red blood cells. *J. Biol. Chem.* 1990; **18**: 10438–10442.
20. Sreerama N, Woody RW. A self-consistent method for the analysis of protein secondary structure from circular-dichroism. *Anal. Biochem.* 1993; **209**: 32–44.
21. Sreerama N, Venyaminov SY, Woody RW. Estimation of the number of alpha-helical and beta-strand segments in proteins using circular dichroism spectroscopy. *Protein Sci.* 1999; **8**: 370–380.
22. Luisi PL, Steinmann-Hofmann B. Activity and conformation of enzymes in reverse micellar solutions. *Meth. Enzymol.* 1987; **136**: 188–216.
23. Souto AL, Ito AS. Tryptophan fluorescence studies of melanotropins in the amphiphile–water interface of reversed micelles. *Eur. Biophys. J.* 2000; **29**: 38–47.
24. Maitra A. Determination of size parameters of water-aerosol OT-Oil reverse micelles from their nuclear magnetic resonance data. *J. Phys. Chem.* 1984; **88**: 5122–5125.
25. Eisenberg D, Weiss RM, Terwilliger TC. The hydrophobic moment detects periodicity in protein hydrophobicity. *Proc. Natl. Acad. Sci. U.S.A.* 1984; **81**: 140–144.
26. Rice P, Longden I, Bleasby A. EMBOSS: the European molecular biology open software suite. *Trends Genet.* 2000; **16**: 276–277.
27. Otvos L Jr, Snyder C, Condie B, Bulet P, Wade J. D. Chimeric antimicrobial peptides exhibit multiple modes of action. *Int. J. Pept. Res. Ther.* 2005; **11**: 29–42.
28. Zelezetsky I, Pacor S, Pag U, Papo N, Shai Y, Sahl HG, Tossi A. Controlled alteration of the shape and conformational stability of alpha-helical cell-lytic peptides: effect on mode of action and cell specificity. *Biochem. J.* 2005; **390**: 177–188.
29. Sreerama N, Venyaminov SY, Woody RW. Estimation of protein secondary structure from circular dichroism spectra: inclusion of denatured proteins with native proteins in the analysis. *Anal. Biochem.* 2000; **287**: 243–251.
30. Sreerama N, Venyaminov SY, Woody RW. Estimation of protein secondary structure from circular dichroism spectra: Comparison of CONTIN, SELCON, and CDSSTR methods with an expanded reference set. *Anal. Biochem.* 2000; **287**: 252–260.
31. Nakanishi K, Berova N, Woody RW. *Circular Dichroism: Principles and Applications*. VCH Publishers: New York, 1994.
32. Lakowicz JR. *Principles of Fluorescence Spectroscopy*. Plenum Press: New York, 1983.
33. Silber JJ, Biasutti A, Abuin E, Lissi E. Interaction of small molecules with reverse micelles. *J. Colloid Interface Sci.* 1999; **82**: 189–252.
34. Albuin E, Lissi E, Duarte R, Silber JJ, Biasutti MA. Solubilization in AOT-water reverse micelles. Effect of the external solvent. *Langmuir* 2002; **18**: 8340–8344.
35. Hirai M, Hirai RK, Sanada M, Iwase H, Mitsuya S. Characteristics of AOT microemulsion structure depending on apolar solvents. *J. Phys. Chem. B* 1999; **103**: 9658–9662.
36. Naoe K, Noda K, Kawagoe M, Imai M. Higher order structure of proteins solubilized in AOT reverse micelles. *Colloids Surf B: Biointerfaces* 2004; **38**: 179–185.
37. Zhou H, Zhou Y. Fold recognition by combining sequence profiles derived from evolution and from depth-dependent structural alignment of fragments. *Proteins* 2005; **58**: 321–328.
38. DeLano WL. *The PyMOL Molecular Graphics System*. DeLano Scientific: San Carlos, 2002; http://www.pymol.org.
39. Matsuzaki K. Magainins as paradigm for the mode of action of pore forming polypeptides. *Biochim. Biophys. Acta* 1998; **1376**: 391–400.
40. Shai Y. From innate immunity to de-novo designed antimicrobial peptides. *Curr. Pharm. Des.* 2002; **8**: 715–725.
41. Dathe M, Wieprecht T. Structural features of helical antimicrobial peptides: their potential to modulate activity on model membranes and biological cells. *Biochim. Biophys. Acta* 1999; **1462**: 71–87.
42. Andreu D, Rivas L. Animal antimicrobial peptides: and overview. *Biopolymers* 1998; **47**: 415–433.
43. Jelinek R, Kolusheva S. Membrane interactions of host-defense peptides studied in model systems. *Curr. Protein Pept. Sci.* 2005; **6**: 103–114.
44. Papo N, Shai Y. Can we predict biological activity of antimicrobial peptides from their interactions with model phospholipids membranes? *Peptides* 2003; **24**: 1693–1703.
45. Ehrenstein G, Lecar H. Electrically gated ionic channels in lipid bilayers. *Q. Rev. Biophys.* 1997; **10**: 1–34.
46. Gazit E, Boman A, Boman HG, Shai Y. Mechanism of interaction of the mammalian antibacterial peptide cecropin P1 with phospholipid vesicles. *Biochemistry* 1995; **34**: 11479–11488.
47. Zhao H, Sood R, Jutila A, Bose S, Fimland G, Nissen-Meyer J, Kinnunen PK. Interaction of the antimicrobial peptide pheromone Plantaricin A with model membranes: implications for a novel mechanism of action. *Biochim. Biophys. Acta* 2006; **1758**: 1461–1474.
48. Barnby-Smith FM. Bacteriocins: applications in food preservation. *Trends Food Sci. Technol.* 1992; **3**: 133–137.
49. Oscáriz J, Pisabarro AG. Classification and mode of action of membrane-active bacteriocins produced by gram-positive bacteria. *Int. Microbiol.* 2001; **4**: 13–19.
50. Chen Y, Ludescher RD, Montville TJ. Influence of lipid composition on pediocin PA-1 binding to phospholipid vesicles. *Appl. Environ. Microbiol.* 1998; **64**: 3530–3532.
51. Atrih A, Rekhif N, Moir AJ, Lebrihi A, Lefebvre G. Mode of action, purification and amino acid sequence of plantaricin C19, an anti-Listeria bacteriocin produced by *Lactobacillus plantarum* C19. *Int. J. Food Microbiol.* 2001; **68**: 93–104.
52. Franz CM, Du Toit M, Olasupo NA, Schillinger U, Holzapfel WH. Plantaricin D, a bacteriocin produced by *Lactobacillus plantarum* BFE 905 ready-to-eat salad. *Lett. Appl. Microbiol.* 1998; **26**: 231–235.

DOI: 10.1002/psc